Monthly Notices
of the
ROYAL ASTRONOMICAL SOCIETY

Mon. Not. R. Astron. Soc. **419,** 806–816 (2012) doi:10.1111/j.1365-2966.2011.19923.x

Post-common envelope binaries from SDSS – XIV. The DR7 white dwarf–main-sequence binary catalogue

A. Rebassa-Mansergas,[1⋆] A. Nebot Gómez-Morán,[2] M. R. Schreiber,[1] B. T. Gänsicke,[3] A. Schwope,[4] J. Gallardo[5] and D. Koester[6]

[1]*Departamento de Física y Astronomía, Universidad de Valparaíso, Avenida Gran Bretana 1111, Valparaíso, Chile*
[2]*Université de Strasbourg, CNRS, UMR7550, Observatoire Astronomique de Strasbourg, 11 Rue de l'Université, F-67000 Strasbourg, France*
[3]*Department of Physics, University of Warwick, Coventry CV4 7AL*
[4]*Astrophysikalisches Inst. Potsdam, An der Sternwarte 16, 14482 Potsdam, Germany*
[5]*Departamento de Astronomía, Universidad de Chile, Casilla 36-D, Santiago, Chile*
[6]*Institut für Theoretische Physik und Astrophysik, University of Kiel, 24098 Kiel, Germany*

Accepted 2011 September 29. Received 2011 September 19; in original form 2011 August 1

ABSTRACT

We present an updated version of the spectroscopic white dwarf–main-sequence (WDMS) binary catalogue from the Sloan Digital Sky Survey (SDSS). 395 new systems are serendipitous discoveries from the spectroscopic SDSS I/II Legacy targets. As part of SDSS Extension for Galactic Understanding and Exploration (SEGUE), we have carried out a dedicated and efficient (64 per cent success rate) search for WDMS binaries with a strong contribution of the companion star, which were under-represented by all previous surveys, identifying 251 additional systems. In total, our catalogue contains 2248 WDMS binaries, and includes, where available, magnitudes from the *GALEX* All Sky Survey in the ultraviolet and from the United Kingdom Infrared Telescope (UKIRT) Infrared Sky Survey (UKIDSS) in the near-infrared. We also provide radial velocities of the companion stars, measured from the SDSS spectroscopy using the Na I λλ 8183.27, 8194.81 absorption doublet and/or the Hα emission. Using an updated version of our spectral decomposition/fitting technique we determine/update the white dwarf effective temperatures, surface gravities and masses, as well as the spectral type of the companion stars for the entire catalogue. Comparing the distributions of white dwarf mass, temperature and companion spectral type, we confirm that our SEGUE survey project has been successful in identifying WDMS binaries with cooler and more massive white dwarfs, as well as earlier spectral types found previously. Finally, we have developed a publicly available interactive online data base for spectroscopic SDSS WDMS binaries containing all available stellar parameters, radial velocities and magnitudes which we briefly describe.

Key words: stars: AGB and post-AGB – binaries: close – binaries: spectroscopic – stars: evolution – stars: low-mass – white dwarfs.

1 INTRODUCTION

Products of common envelope evolution play important roles in many areas of modern astronomy, e.g. stellar black hole binaries as laboratories for general relativity, double-degenerate white dwarf binaries as potential progenitors of Type Ia supernovae, or double-degenerate neutron star binaries as progenitors of short gamma-ray bursts. The fundamental concept of the formation of such systems is well established: once the more massive star in a main-sequence binary evolves into a red giant, unstable mass transfer is initiated at a rate that exceeds the Eddington limit of the companion star, and leads to the formation of a common envelope around the giant core and its less massive main-sequence companion (Paczynski 1976; Webbink 1984; Iben & Tutukov 1986; Iben & Livio 1993). Drag forces between the binary components and the material of the envelope lead to a dramatic decrease of the binary separation, and the orbital energy released due to the shrinkage of the orbit eventually expels the envelope exposing a post-common envelope binary (PCEB).

PCEBs continue to evolve to even shorter orbital periods through angular momentum loss given by magnetic braking and/or gravitational wave emission, and may either undergo a second common envelope, leading to double-degenerate PCEBs, or enter a semidetached state and appear as cataclysmic variables, super-soft X-ray sources or X-ray binaries. Because of the complex physical

⋆E-mail: arebassa@dfa.uv.cl

processes involved in the common envelope evolution, our understanding of this important phase is still very poor, and severely underconstrained by observations.

Among the variety of PCEBs, white dwarf–main-sequence (WDMS) binaries are intrinsically the most common, and structurally the simplest population, and hold a strong promise to provide crucial observational input that is necessary for improving the theory of close binary evolution (Schreiber & Gänsicke 2003). WDMS binaries descend from main-sequence binaries, where the primary has a mass $\lesssim$10 $M_\odot$. In the majority of cases ($\sim$3/4), the initial main-sequence binary separation is large enough for the white dwarf precursor to evolve in the same way as a single star (de Kool 1992; Willems & Kolb 2004), and consequently the orbital period of these systems will increase because of the mass loss of the primary. In the remaining $\sim$1/4 of the cases, the system enters a common envelope, leading to a drastically shorter orbital period. The orbital period distribution of the entire population of WDMS binaries is therefore expected to be strongly bimodal, with the short orbital period PCEBs clearly separated from the long orbital period WDMS binaries that did not undergo common envelope evolution. This seems to be confirmed by a recent high-resolution imaging campaign of 90 white dwarfs with known or suspected low-mass stellar and substellar companions (Farihi, Becklin & Zuckerman 2005; Farihi, Hoard & Wachter 2010).

The Sloan Digital Sky Survey (SDSS; York et al. 2000; Adelman-McCarthy et al. 2008; Abazajian et al. 2009) has been very efficient at identifying large numbers of WDMS binaries (Raymond et al. 2003; Silvestri et al. 2007; Heller et al. 2009), with 1602 systems in Data Release 6 (DR6) (Rebassa-Mansergas et al. 2010). Intense radial velocity studies have led to the identification of a large number of PCEBs among the sample of SDSS WDMS binaries (Rebassa-Mansergas et al. 2007; Schreiber et al. 2008, 2010). A few examples of the work already done with both the entire sample of SDSS WDMS binaries and the subset of systems identified to be PCEBs are the identification of many eclipsing PCEBs, important for testing the models of stellar structure (Nebot Gómez-Morán et al. 2009; Pyrzas et al. 2009, 2011; Parsons et al. 2010, 2011); observational constraints on the efficiency of the common envelope (Zorotovic et al. 2010; De Marco et al. 2011); strong evidence for a discontinuity in the strength of magnetic braking near the fully convective boundary (Schreiber et al. 2010); and an unambiguous demonstration that the majority of low-mass (He-core) white dwarfs are formed in binaries (Rebassa-Mansergas et al. 2011).

Here, we present the final catalogue of WDMS binaries identified from SDSS (DR7) spectroscopy, discuss the global properties of the 2248 systems and describe a public interactive online data base of spectroscopic SDSS WDMS binaries.

2 FROM SDSS I TO SDSS II

During its first phase of operations, from 2000 to 2005, SDSS I mainly obtained spectra of galaxies and quasars selected from 5700 deg^2 of imaging. The corresponding data largely dominate the DR6 of SDSS (Adelman-McCarthy et al. 2008). From 2005 to 2008, SDSS II carried out three distinct surveys:

(i) the Sloan Legacy Survey, which completed the original (mainly extragalactic) SDSS I imaging and spectroscopic goals;

(ii) the SDSS Extension for Galactic Understanding and Exploration (SEGUE; Yanny et al. 2009), which probed the structure and history of the Milky Way, obtaining additional imaging over a large range of Galactic latitudes as well as spectroscopy for $\sim$240 000 stars;

(iii) the Sloan Supernova Survey, which carried out repeat imaging of the 300 deg^2 southern equatorial stripe to discover and measure supernovae and other variable objects.

The final data product of SDSS I and most of SDSS II is DR7 (Abazajian et al. 2009). The different design of SDSS II and in particular the inclusion of a dedicated target selection for WDMS binaries in SEGUE significantly changes the resulting WDMS binary star content compared to DR6. Below we review the two main channels that led to WDMS binary spectra taken by SDSS.

2.1 WDMS in SDSS I

The main science driver of SDSS I has been to acquire spectroscopy for magnitude-limited samples of galaxies (Strauss et al. 2002) and quasars (Richards et al. 2002). Because of their composite nature, WDMS binaries form a 'bridge' in colour space that connects the white dwarf locus to that of low-mass stars (Smolčić et al. 2004). The blue end of the bridge, characterized by WDMS binaries with hot white dwarf and/or late-type companions, strongly overlaps with the colour locus of quasars, and was therefore intensively targeted by SDSS spectroscopy. In contrast, the red end of the bridge is totally dominated by WDMS binaries containing cool white dwarfs, and excluded from the quasar programme. Some additional WDMS binaries were directly selected for SDSS spectroscopy following the selection criteria of Raymond et al. (2003) and Silvestri et al. (2006). These criteria are based on the idea that a WDMS binary needs to be both red (main sequence) and blue (white dwarf), which is only true for a relatively small fraction of possible WDMS binary colours. In particular, systems in which one of the stellar components dominates the emission are excluded. In summary, the overall SDSS I spectroscopic sample of WDMS binaries (Raymond et al. 2003; Silvestri et al. 2007; Heller et al. 2009; Rebassa-Mansergas et al. 2010) is heavily biased against WDMS binaries containing cold white dwarfs and/or early-type secondaries, just as Schreiber & Gänsicke (2003) found for the pre-SDSS sample.

2.2 WDMS in SDSS II

Within SDSS II, the Legacy project is expected to identify WDMS binaries with similar properties and at a similar rate as within SDSS I. However, SEGUE included a small number of projects targeting specific classes of objects, and we have developed a colour selection to find WDMS binaries containing either cool white dwarfs and/or early M-dwarf/late K-dwarf companions, i.e. a population of WDMS binaries that has been consistently under-represented in the SDSS I and all the previous surveys.

To that end we simulated *ugriz* colours of WDMS binaries spanning a broad range in white dwarf effective temperatures (T_{wd} = 6000–40 000 K) and companion star spectral types (K0–M6) (see also Schreiber, Nebot Gómez-Morán & Schwope 2007). Absolute Johnson *UBVRI* magnitudes for white dwarfs and for M/K dwarfs were taken from an updated version of Bergeron, Wesemael & Beauchamp (1995) and Pickles (1998), respectively. The combined *UBVRI* magnitudes were converted to *ugriz* using the empirical colour transformations of Jordi, Grebel & Ammon (2006). Fig. 1 shows the loci of the synthetic SDSS WDMS binary colours in three different colour–colour diagrams ($u-g$ versus $g-r$, $g-r$ versus $r-i$ and $r-i$ versus $i-z$) and demonstrates that systems dominated by the thermal flux of the secondary star can

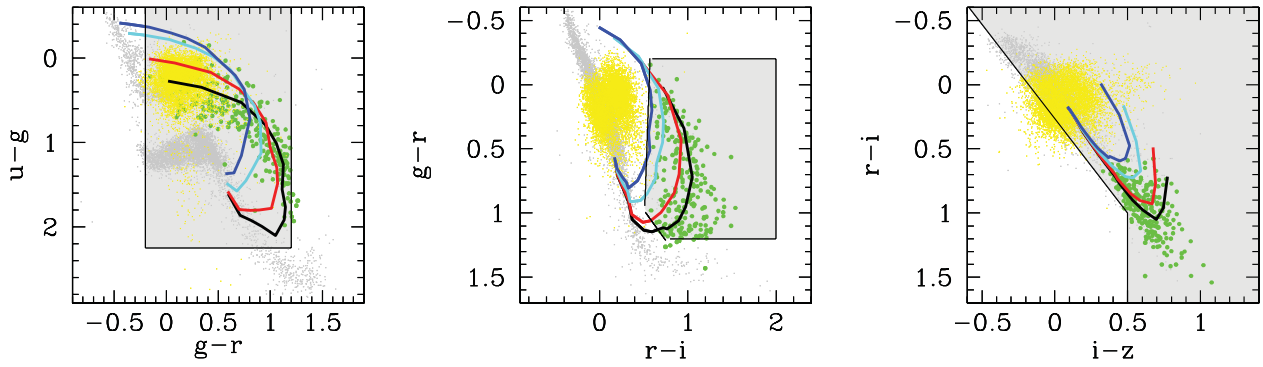

Figure 1. Synthetic WDMS binary colours in the $u-g$ versus $g-r$ (left-hand panel), $g-r$ versus $r-i$ (centre panel) and $r-i$ versus $i-z$ (right-hand panel) colour–colour diagrams. Colour tracks are shown for WDMS binaries containing secondary star spectral types K0 to M6, as well as white dwarf effective temperatures of 40 000 K (blue), 30 000 K (cyan), 20 000 K (red) and 10 000 K (black). Colours for quasars and single main-sequence stars are shown as yellow and grey dots, respectively. In grey-shaded area, we represent our selection criteria specially designed to identify WDMS binaries containing cold white dwarfs and/or early-type companions. The resulting sample of WDMS binaries identified by our selection criteria is represented by green dots.

be separated from quasars (yellow dots), main-sequence stars (grey dots) and WDMS binaries dominated by the thermal flux of the white dwarf by applying the following cuts:

$$\begin{aligned} &u-g<2.25, \qquad g-r>-19.78(r-i)+11.13,\\ &g-r>-0.2, \qquad g-r<0.95(r-i)+0.5,\\ &g-r<1.2, \qquad i-z>0.5 \quad \text{for} \quad r-i>1.0,\\ &r-i>0.5, \quad i-z>0.68(r-i)-0.18 \quad \text{for} \quad r-i<=1.0,\\ &r-i<2.0, \qquad 15<g<20. \end{aligned} \tag{1}$$

These selection criteria (grey shaded in Fig. 1) optimize the identification of WDMS binaries consisting of both cold white dwarfs and early-type secondaries.

3 THE DR7 SDSS WDMS BINARY CATALOGUE

In this section we describe the final spectroscopic DR7 WDMS binary catalogue. It is important to keep in mind that the complete DR7 catalogue will be formed by WDMS binaries identified in SDSS I and the Legacy survey in SDSS II, and by WDMS binaries identified within our SEGUE survey. In what follows we will denote the former as the SDSS I/II WDMS binary sample and the latter as the SEGUE WDMS binary sample.

We first present the outcome of the dedicated SEGUE WDMS binary survey and then provide a brief review of the WDMS binary search algorithm that we apply to the entire SDSS DR7 spectroscopic data set (for details see Rebassa-Mansergas et al. 2010). Finally we estimate the completeness of the final SDSS DR7 spectroscopy WDMS binary catalogue.

3.1 The SEGUE WDMS binary sample

In 2005 October, SEGUE incorporated the colour selection given in the previous section with the goal of targeting on average five, and at most 10 WDMS binary candidates per plate pair. In addition to the colour criteria we requested clean photometry for the selection of our targets. By the end of SDSS II in mid-2008, 116 plate pairs and eight single plates including our WDMS binary target selection were observed in SEGUE (Table 1). However, during the early stages of SEGUE, 14 plate pairs and two single plates (those <2377 in Table 1) considered dereddened *ugriz* magnitudes before applying our colour selection, resulting in a number of single (unreddened) foreground M dwarfs being observed.

Using the DR7 CasJobs interface (Li & Thakar 2008),[1] we selected all point sources within the footprint defined by the plates listed in Table 1 that have clean photometry and satisfy our colour selection. This search resulted in 10 505 unique point sources, of which 429 were followed up spectroscopically. Among the 429 spectroscopic objects, we identified 274 as WDMS binaries, corresponding to a 'hit rate' of $\simeq$64 per cent. Two additional WDMS binaries (SDSS J135643.56−085808.9 and SDSS J135930.96−101029.7) were found on plate 2716 that has not been published via DR7, and 15 objects were found on the plates done with dereddened magnitudes that do not satisfy our colour criteria. Cross-matching these 291 WDMS binaries with our DR6 catalogue (Rebassa-Mansergas et al. 2010), we found that 40 systems had SDSS spectroscopy obtained as part of SDSS I/II, implying that $\sim$15 per cent of the targeted systems are duplicates. Hence, the number of genuinely new systems identified within SEGUE is 251.

The loci of the SEGUE WDMS binaries are shown in Fig. 1 in green; a few systems outside our colour selection (grey-shaded area) are those found on the plates done with dereddened magnitudes. WDMS binaries identified by our SEGUE survey are flagged as such in the last column of Table A6.

3.2 The final DR7 WDMS binary sample

We searched all new $\sim$0.4 million spectra from SDSS DR7 for WDMS binaries following the template-fitting method outlined in Rebassa-Mansergas et al. (2010). We used as templates 163 previously identified WDMS binaries from Rebassa-Mansergas et al. (2010), spanning the whole range of white dwarf effective temperatures and companion star spectral types, and calibrated the constraints in both χ^2 and signal-to-noise ratio for each of them. We then visually inspected the selected WDMS binary candidates and divided the systems in three different categories: WDMS binary, white dwarf and M dwarf. Given that visual inspection of WDMS binaries in which one of the stellar components dominates the SDSS spectrum can be misleading, we complemented the SDSS data with the photometry provided by the *Galaxy Evolution Explorer* (*GALEX*; Martin et al. 2005; Morrissey et al. 2005) and the United Kingdom Infrared Telescope (UKIRT) Infrared Sky Survey (UKIDSS; Dye et al. 2006; Hewett et al. 2006; Lawrence et al. 2007;

[1] http://casjobs.sdss.org/CasJobs/

Table 1. The list of 116 plate pairs and eight single plates with WDMS target selection that have been observed in SEGUE.

2303/2318	2315/2330	2382/2402	2397/2417	2459/2474	2555/2565	2667/2671	2682/2700	2801/2822	2854/2869	2888/2913	2899/2924	2909/2934	2336
2304/2319	2316/2331	2383/2403	2441/2443	2537/2545	2556/2566	2668/2672	2683/2701	2803/2824	2855/2870	2889/2914	2901/2926	2910/2935	2337
2305/2320	2317/2332	2384/2404	2442/2444	2538/2546	2557/2567	2669/2673	2689/2707	2805/2826	2856/2871	2890/2915	2902/2927	2911/2936	2475
2306/2321	2334/2339	2386/2406	2445/2460	2539/2547	2558/2568	2670/2674	2690/2708	2806/2827	2857/2872	2891/2916	2903/2928	2938/2943	2552
2307/2322	2335/2340	2387/2407	2446/2461	2540/2548	2559/2569	2676/2694	2714/2729	2807/2828	2858/2873	2893/2918	2904/2929	2939/2944	2620
2308/2323	2378/2398	2389/2409	2447/2462	2541/2549	2621/2627	2677/2695	2724/2739	2812/2833	2859/2874	2894/2919	2905/2930	2940/2945	2865
2310/2325	2379/2399	2390/2410	2449/2464	2551/2561	2622/2628	2678/2696	2797/2818	2849/2864	2861/2876	2895/2920	2906/2931	2941/2946	2866
2312/2327	2380/2400	2393/2413	2452/2467	2553/2563	2623/2629	2680/2698	2798/2819	2852/2867	2862/2877	2897/2922	2907/2932	2963/2965	2942
2313/2328	2381/2401	2394/2414	2457/2472	2554/2564	2624/2630	2681/2699	2800/2821	2853/2868	2887/2912	2898/2923	2908/2933		

Warren et al. 2007) and searched for blue (red) excess in the spectra classified as M dwarf (white dwarf). All systems in which we detected either a blue or red excess were reclassified as WDMS binaries. Subsequently we inspected the SDSS images of our selected WDMS binary candidates and excluded objects with morphological problems in their images. Finally, we cross-checked our list of WDMS binaries with the 1602 systems from DR6 (Rebassa-Mansergas et al. 2010) as well as the 251 SEGUE WDMS binaries identified in Section 3.1. 390 genuinely new WDMS binaries were found in the Legacy part of DR7, which, in addition to the 251 systems identified in the SEGUE survey, bring the total number of new WDMS binaries in DR7 to 641.

3.3 Catalogue completeness

Here, we analyse the completeness of the SEGUE WDMS binary sample within the survey footprint defined by the 240 spectroscopic plates listed in Table 1, as well as the completeness of the SDSS I/II WDMS binary sample.

We define the completeness of our SEGUE sample as the number of SEGUE WDMS binaries found by our template-fitting method (Section 3.2) that have colours satisfying our selection criteria (equation 1) divided by the number of all 274 SEGUE WDMS binaries found in Section 3.1. We find a completeness of 100 per cent, i.e. all SEGUE WDMS binaries were correctly identified by our template-fitting method.

To calculate the completeness of the SDSS I/II WDMS binary sample is not straightforward, as it becomes necessary to analyse the entire Legacy footprint. Such an endeavour is far away from the scope of this paper; however, we can estimate the completeness by analysing photometric areas representative of the SDSS I/II WDMS binary population. For this purpose, we used the three colour regions defined by Rebassa-Mansergas et al. (2010). For the DR6 WDMS binary catalogue this resulted in a completeness of $\gtrsim$ 98 per cent (see section 3 in Rebassa-Mansergas et al. 2010). Here, we identified only five additional WDMS binaries to the 390 identified in Section 3.2 that were not found by our template-fitting method, implying a completeness of $\gtrsim$98 per cent. The five systems are SDSS J001846.79+000237.6, SDSS J020756.15+214027.4, SDSS J133902.65+104136.3, SDSS J150538.90+563353.2 and SDSS J224122.87+010608.6. The spectra of these five objects are completely dominated by the flux of the secondary star, and only a mild blue excess is seen in the blue part of the spectra. Adding these five objects to our SDSS I/II sample increases the number of new spectroscopic WDMS binaries to 395. The *total* number of WDMS binaries in the entire SDSS DR7 thus increases to 2248: 251 form the SEGUE WDMS binary sample and 1997 form the SDSS I/II WDMS binary sample (1602 within DR6 identified by Rebassa-Mansergas et al. 2010, 395 identified in this work). Fig. 2 provides the position of the complete SDSS WDMS binary catalogue both in Galactic and equatorial coordinates, and an excerpt of the complete list can be found in Table A2.

In summary, we conclude that we are confident to have identified nearly all ($\gtrsim$98 per cent) WDMS binaries within the entire DR7 spectroscopic data release, and that our SEGUE survey has been very efficient in identifying WDMS binaries within a colour space that has so far been neglected.

4 CHARACTERIZATION OF THE SDSS WDMS BINARY POPULATION

With more than 2000 systems and being $\gtrsim$98 per cent complete, our spectroscopic DR7 SDSS WDMS binary catalogue represents so far

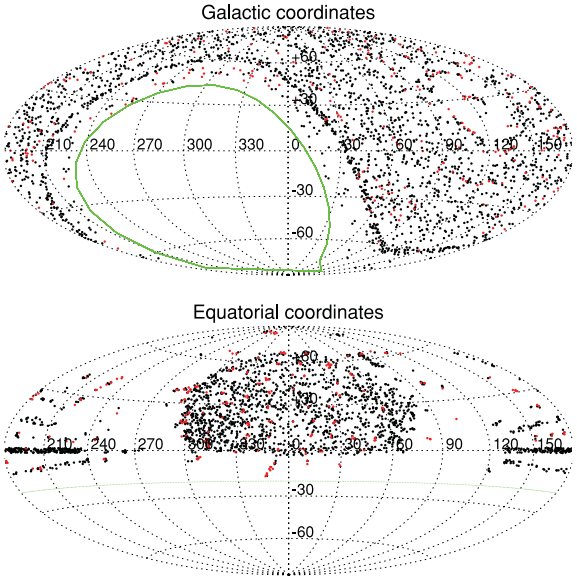

Figure 2. Position of SDSS I/II (black) and SEGUE (red) WDMS binaries in Galactic and equatorial coordinates.

the largest and most homogeneous sample of compact binary stars. We here provide stellar parameters, distances, radial velocities and magnitudes for the complete DR7 SDSS WDMS binary catalogue. Special attention is taken to characterize the differences between the SEGUE and the SDSS I/II WDMS binary samples.

4.1 Ultraviolet and near-infrared magnitudes

We cross-correlated our list of WDMS binaries with *GALEX* GR 6 (Martin et al. 2005; Morrissey et al. 2005), which provides an updated processing of the *GALEX* data compared to GR 4, which we used in Rebassa-Mansergas et al. (2010). Therefore, the *GALEX* ultraviolet magnitudes in this paper supersede those published in our latest WDMS binary catalogue. We also cross-correlated all WDMS binaries with UKIDSS DR6 (Lawrence et al. 2007; Warren et al. 2007) to obtain near-infrared *yJHK* magnitudes. Where available, *GALEX* and UKIDSS data are given in Table A4 together with the *ugriz* SDSS magnitudes.

4.2 Radial velocities

We measured radial velocities from the available SDSS subspectra,[2] as well as from the average SDSS spectra. Radial velocities were measured fitting two Gaussians of fixed separation but free individual widths and amplitudes to the Na I λλ 8183.27, 8194.81, and/or a Gaussian to the Hα emission line (see Rebassa-Mansergas et al. 2008 for details). See Table A3 for the heliocentric corrected dates of the observations and the corresponding radial velocities.

4.3 Stellar parameters

In order to determine the stellar parameters of our SDSS WDMS binaries we used the spectral decomposition/fitting routine described in Rebassa-Mansergas et al. (2007, 2010). Intensive tests of our white dwarf fitting procedure using SDSS spectra of single white dwarfs revealed that we overestimated the errors on the white dwarf parameters by a factor of ∼2 in our previous SDSS WDMS binary studies (Rebassa-Mansergas et al. 2011); we hence refitted the spectra of all SDSS WDMS binaries to obtain more realistic uncertainties of the white dwarf parameters.

Our fitting routine follows a two-step procedure. First, a given SDSS WDMS binary spectrum is fitted with a two-component model using the M-dwarf and white dwarf templates of Rebassa-Mansergas et al. (2007). We used an evolution strategy (Rechenberg 1994) to decompose the WDMS binary spectra into their two individual stellar components. In brief, this method optimizes a fitness function, in this case a weighted χ^2, and allows an easy implementation of additional constraints, such as e.g. the inclusion of a Gaussian fit to the Balmer emission lines. From the converged white dwarf plus M-dwarf template fit to each WDMS spectrum, we recorded the spectral type of the secondary star, as well as the flux scaling factor between the M-star template and the observed spectrum. Subsequently, the best-fitting M-dwarf template, scaled by the appropriate flux scaling factor, is subtracted from the SDSS spectrum, and the residual white dwarf spectrum is fitted with a model grid of DA white dwarfs (Koester et al. 2005). More specifically, we fit the normalized Hβ to Hϵ line profiles to determine the white dwarf effective temperature and surface gravity ($\log g$). We exclude Hα from this fit as it is in many cases contaminated by the flux residuals of the M dwarf. The equivalent widths of the Balmer lines go through a maximum near $T_{\rm eff} = 13\,000$ K, with the exact value being a function of $\log g$. Therefore, $T_{\rm eff}$ and $\log g$ determined from Balmer line profile fits are subject to an ambiguity, often referred to as 'hot' and 'cold' solutions. This degeneracy is broken fitting also the entire white dwarf spectrum (continuum plus lines), excluding only wavelengths >7150 Å (again to minimize contamination by flux residuals from M-dwarf companion). The slope of the white dwarf spectrum is mostly sensitive to $T_{\rm eff}$, and the best-fitting value from the entire spectrum is then used to choose between the hot and cold solutions. All fits are visually inspected, and, where available, the choice of the hot versus cold solution is further guided by the comparison of the predicted ultraviolet fluxes to *GALEX* measurements. From an empirical spectral type–radius relation for M dwarfs (Rebassa-Mansergas et al. 2007) and a mass–radius relation for white dwarfs (Bergeron, Wesemael & Beauchamp 1995; Fontaine, Brassard & Bergeron 2001), we calculate then the radius of the secondary star and the mass and the radius of the white dwarf, respectively. From the radii and the flux scaling factors between the WDMS binary components and the white dwarf models and main-sequence star templates, we finally obtain two independent distances.

From the total list of parameters we selected a 'clean' list by applying the following restrictions. As a systematic increase in the surface gravity for white dwarfs below ∼12 000 K has been observed in recent white dwarf studies (e.g. Koester et al. 2009), we only consider white dwarf masses and gravities if the white dwarf temperature exceeds this value. In order to avoid contamination from unreliable stellar parameters, we additionally only consider objects with a relative error of less than 15 per cent in the white dwarf parameters. For the SDSS I/II WDMS binary sample, this resulted in 1378, 1278 and 579 WDMS binaries in the distributions of white dwarf effective temperatures, surface gravities and masses, respectively (top panels in Fig. 3, black). For the SEGUE sample the distributions contain 143, 144 and 79 WDMS binaries, respectively (bottom panels in Fig. 3, black). The spectral types of the secondary stars are directly determined from the spectral template fitting. For the SDSS I/II and SEGUE sample, 1768 and 251 WDMS binaries

[2] Each SDSS spectrum is the result of averaging several (typically three) individual exposures, or subspectra.

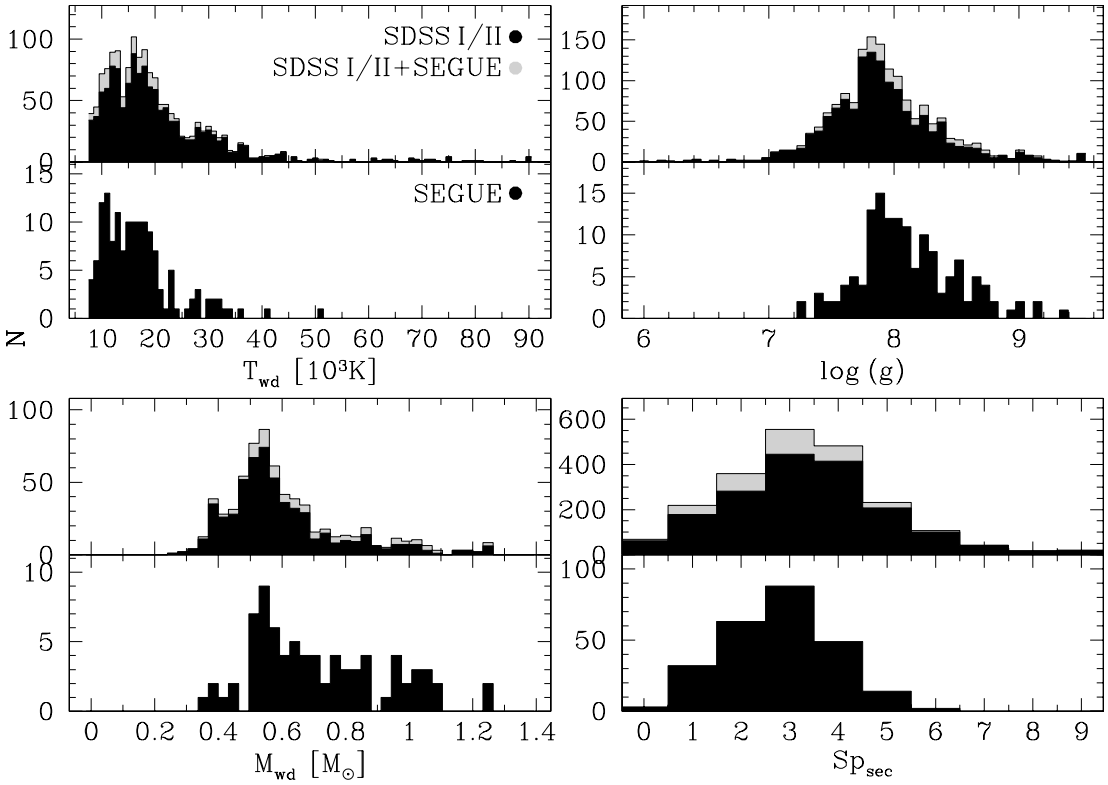

Figure 3. Distributions of white dwarf effective temperatures (top left), surface gravities (top right) and masses (bottom left), and spectral type of the companions (Sp_{sec}, bottom right). Top panels show in black and grey the SDSS I/II and SDSS I/II plus SEGUE WDMS binary distributions. Bottom panels show in black the parameter distributions of the SEGUE WDMS binary sample.

containing M dwarfs have reliable spectral types, respectively, and are included in the distribution.

The stellar parameter distributions of the complete SDSS WDMS binary sample (SDSS I/II plus SEGUE) are shown in grey in the top panels of Fig. 3 and the cumulative distributions of the SDSS I/II and the SEGUE sample are shown in Fig. 4.

It is very clear that the stellar parameters of the SDSS I/II WDMS binary sample differ from those in the SEGUE WDMS binary population (black distributions in Fig. 3). Kolmogorov–Smirnov and χ^2 (in case of the spectral type distributions) tests applied to the cumulative stellar parameter distributions in both subsamples gave probabilities $<10^{-4}$ in all cases, clearly indicating that the two populations are different. These differences have a straightforward explanation. WDMS binaries detected within our SEGUE survey (Section 2.2) are by definition of the selection criteria considerably less blue than WDMS binaries from SDSS I/II. This favours the detection of WDMS containing cold and massive (and hence small) white dwarfs and early M spectral types.

(i) The upper-left panel of Fig. 4 shows the white dwarf effective temperature cumulative distributions. Inspecting the figure it becomes clear that the number of cold white dwarfs is significantly higher in our SEGUE WDMS binary sample.

(ii) The upper-right and lower-left panels of Figs 3 and 4 clearly show that the SEGUE sample contains more systems with massive white dwarfs with a higher surface gravity.

(iii) The secondary star spectral type distributions are provided in the bottom-right panel of Figs 3 and 4. As a natural consequence of our selection criteria (Section 2.2), the sample of SEGUE

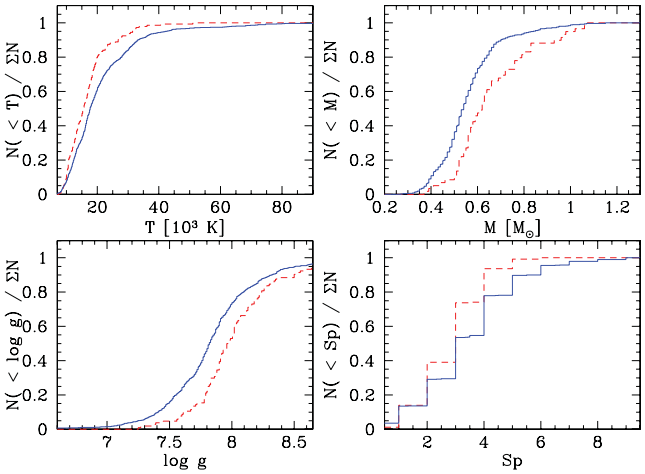

Figure 4. White dwarf effective temperature (top left), surface gravity (top right) and mass (bottom left), and spectral type of the companion (Sp_{sec}, bottom right) cumulative distributions obtained from the SDSS I/II sample of WDMS binaries (solid blue lines), and those WDMS binaries identified within SEGUE (red dashed lines).

WDMS binaries contains more secondary stars of spectral types M0–M6.

The comparison of the SDSS I/II and SEGUE WDMS binary samples clearly demonstrates that our selection criteria (equation 1) were efficient at identifying WDMS binaries containing

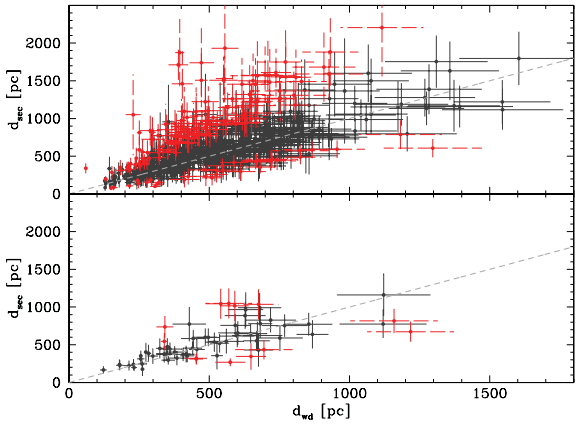

Figure 5. Secondary star distances as a function of white dwarf distances for a subsample of 575 SDSS I/II (top panel) and 65 SEGUE (bottom panel) WDMS binaries in which the white dwarf distance relative error is less than 15 per cent. In red 1.5σ outliers from $d_{\rm sec} = d_{\rm WD}$ (grey dashed line).

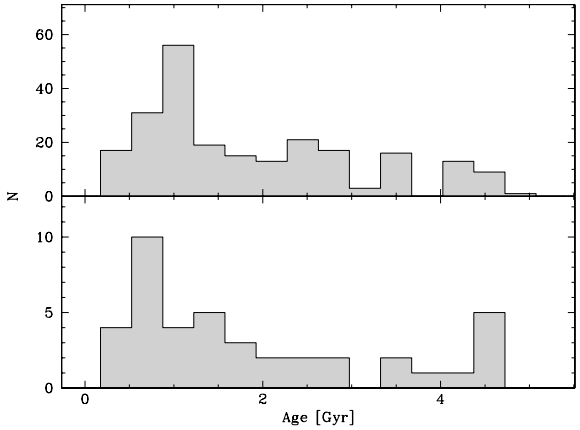

Figure 6. Distribution of WDMS binary ages for a subsample of 231 SDSS I/II (top panel) and 41 SEGUE (bottom panel) systems. See Section 4.4 for details.

cold/massive white dwarfs and early-type secondary stars, i.e. a population that has been under-represented by all previous surveys.

4.4 Distances

Two independent distances have been determined for each system from the flux scaling factors between the model (template) fit and the observed fluxes, and the use of a mass–radius relation for white dwarfs and an empirical spectral type–radius relation for M dwarfs. The obtained distances are compared here. To avoid statistical and systematic uncertainties in the comparison, we require the relative error in the white dwarf distances ($d_{\rm WD}$) to be less than 15 per cent, the effective temperature of the white dwarfs to exceed 12 000 K, and exclude systems with indications for both components being resolved on the SDSS image.[3] The relative error in the secondary star distance ($d_{\rm sec}$) is dominated by the scatter in the empirical M-dwarf spectral type–radius relation (Rebassa-Mansergas et al. 2007, see their fig. 7), which represents an intrinsic uncertainty rather than a statistical error in the fit, and we consequently do not apply any error cut in $d_{\rm sec}$. Fig. 5 provides $d_{\rm WD}$ as a function of $d_{\rm sec}$ for the resulting 575 SDSS I/II (top panel) and 65 SEGUE (bottom panel) WDMS binaries.

An effect previously identified by Schreiber et al. (2008) and Rebassa-Mansergas et al. (2010) can be seen in the SDSS I/II sample (Fig. 5, top panel): for 27.0 ± 2 per cent of the systems the two distance estimates disagree at a 1.5σ significance level (red points in Fig. 5), with the vast majority (21.4 ± 2 per cent) of these having $d_{\rm sec} > d_{\rm WD}$ outliers. Only relatively few systems are found significantly below $d_{\rm sec} = d_{\rm WD}$ (5.6 ± 1 per cent). Conversely, the fraction of 1.5σ outliers in the SEGUE WDMS binary sample (Fig. 5, bottom panel) not only decreases but also is almost identical above (10.7 ± 3.5 per cent) and below (9.2 ± 3.6 per cent) $d_{\rm sec} = d_{\rm WD}$.

Rebassa-Mansergas et al. (2007) interpreted the $d_{\rm sec} > d_{\rm WD}$ outlier effect as resulting from magnetic activity affecting the surface of the secondary stars. If this was the case, the fraction of active secondary stars in the SEGUE WDMS binary sample should be significantly smaller. One might intend to interpret this as being a consequence of the SEGUE WDMS binaries being, on average, older (since the white dwarfs forming the SEGUE sample are systematically cooler, see Fig. 4), as it has been demonstrated that older M dwarfs are systematically less active (West et al. 2008). However, as we are considering only systems with white dwarf effective temperatures exceeding 12 000 K (Fig. 5), this age-effect is expected to be negligible.

To investigate this quantitatively, we have estimated the ages of the WDMS binaries of the SDSS I/II and SEGUE subsamples in Fig. 5 and compared them to the activity lifetimes of West et al. (2008). The total age of each system is given by the sum of the white dwarf cooling age and the main-sequence lifetime of the white dwarf progenitor. White dwarf cooling ages were calculated from the cooling tracks of Althaus & Benvenuto (1997). Main-sequence progenitor lifetimes were obtained from the equations of Tuffs et al. (2004, see their appendix), where the main-sequence progenitor masses were calculated using the initial-to-final mass relation by Catalán et al. (2008). A relatively large percentage of WDMS binaries are PCEBs (Schreiber et al. 2010), for which the initial-to-final mass relation for single white dwarfs is generally not valid. However, Zorotovic, Schreiber & Gänsicke (2011, their fig. 9) demonstrated that this relation is a good approximation for PCEBs between 0.55 and 0.8 $M_{\odot}$, as the core of the progenitors of such white dwarfs is almost entirely developed at the onset of common envelope evolution. We therefore considered only systems containing white dwarfs with masses in this range. The estimated ages are compared to the activity lifetimes of West et al. (2008) in Table 2, where we provide the percentages of systems with ages above and below the activity lifetime for different spectral types. For completeness, the estimated ages are also illustrated in Fig. 6. The fractions of systems that should be active according to their age are very similar for WDMS binaries in both samples (Table 2), i.e. 28 ± 3 per cent (SDSS I) and 31 ± 7 per cent (SEGUE). Thus, the two samples should also contain approximately the same number of $d_{\rm sec} > d_{\rm WD}$ outliers if those are caused by activity. This is apparently not the case (Fig. 5) and we conclude that the SEGUE data question our previous interpretation of magnetic activity causing the distance disagreement, and that this discrepancy remains an unsolved issue. Using model spectra (e.g. PHOENIX; Hauschildt & Baron 1999) instead of M-dwarf templates in the decomposition/fitting of the SDSS WDMS binary spectra and comparing both results may provide useful insights (e.g. Heller et al. 2009).

[3] The flux contribution of one or both stars in a resolved WDMS binary spectrum is likely to be underestimated and this translates into an underestimated flux scaling factor and overestimated distance.

Table 2. Percentage of WDMS binary ages for the SDSS I/II and SEGUE samples defined in Section 4.4 that are above and below the activity lifetimes estimated by West et al. (2008) as a function of spectral type.

Spectral type	Activity lifetime	SDSS I/II		SEGUE	
		>activity lifetime	<activity lifetime	>activity lifetime	<activity lifetime
	(Gyr)	(per cent)	(per cent)	(per cent)	(per cent)
M0	0.8 ± 0.6	60	40	–	–
M1	0.4 ± 0.4	6	94	0	100
M2	1.2 ± 0.4	42	58	37	64
M3	2.0 ± 0.5	57	43	69	31
M4	4.5 ± 0.5	97	3	100	0
M5	7.0 ± 0.5	100	0	100	0
M6	7.0 ± 0.5	100	0	–	–

5 THE SDSS WDMS BINARY ONLINE DATA BASE

We have presented an updated version of the spectroscopic SDSS WDMS binary catalogue incorporating 646 new systems from the DR7 spectroscopic data base (Section 3). A significant fraction of the new systems (251) have been identified by our SEGUE WDMS binary survey (Section 2.2). The entire DR7 SDSS WDMS binary catalogue contains now 2248 objects, each of them associated with a large number of stellar parameters, radial velocities and photometric magnitudes. Given a large amount of available information we developed a Structured Query Language (SQL) interactive online data base for spectroscopic SDSS WDMS binaries. This data base is open for the general public; however, permission to update the data base will be restricted to our team.

The data base allows the user to search for information in three different ways and is based on six different tables that form the SQL's data base. In the following we provide instructions on how to use the interactive SDSS WDMS binary data base and give details on the content of each table. More detailed information and examples can be found on the web page http://www.sdss-wdms.org/.

5.1 Description of tables

Each of the SDSS WDMS binaries in our catalogue has been given an identification number (ID), ranging from 1 to 2248. This ID is unique for each object. In addition, we have named our systems by their International Astronomical Union (IAU) name, i.e. SDSS JHHMMSS.SS±DDMMSS.S, as well as by an abbreviated form, i.e. SDSS JHHMM ± DDMM. On the SQL's data base the table 'obj_iau_name' contains the ID and the IAU name of the 2248 WDMS binaries, the table 'object' contains both the ID and the abbreviated names. The ultraviolet *GALEX* DR6, the *ugriz* SDSS and the near-infrared UKIDSS DR6 magnitudes plus photometric errors, as well as the right ascensions and declinations of our targets are stored in the table 'magnitudes'. The measured Na I absorption doublet and Hα emission radial velocities and corresponding errors, together with the heliocentric corrected dates of the observations can be found in the table 'rv'. To these radial velocities we added the measurements presented in Schreiber et al. (2010) and Nebot Gómez-Morán et al. (2011). The stellar parameters together with the SDSS identifiers (i.e. Modified Julian Date, MJD, plate, PLT and fibre, FIB), the distances and the WDMS binary spectral types are given in the table 'wdms'. Finally the average stellar parameters (for several objects multiple SDSS spectra are available) and those derived from additional follow-up observations performed by us are provided in the table 'mean_param'. The six tables are linked using the IAU names and excerpts of each table can be found in Appendix A.

5.2 Queries

The data base just described can be searched in three different ways.

(i) *Search by object*. This option allows the user to obtain all available information for a specific object or a list of objects using either the IAU or the abbreviated identifiers. The provided information for each system includes *ugriz* SDSS, ultraviolet DR6 *GALEX* and near-infrared DR6 UKIDSS magnitudes (when available), the binary and stellar parameters as well as the SDSS image and spectrum, the two-component fits to the SDSS WDMS binary spectrum, and the model fit to the residual white dwarf spectrum as obtained from our decomposition/fitting routine.

(ii) *Search by parameter*. The user may define constraints on a chosen set of parameters to obtain a list of objects that satisfy user-defined conditions. Such constraints can be applied to all the stellar parameters, magnitudes and radial velocities, as well as coordinates and PCEB orbital periods. To provide access to the results of our follow-up studies, we have additionally defined the following parameters: (1) 'sigma', set to 3 or 4 depending on whether we detect 3σ or 4σ radial velocity variations, set to 0 when no radial velocity variations are detected, set to -1 when no information is available (in other words 'sigma' = 3, 4 stands for a PCEB, 'sigma' = 0 for a wide WDMS binary candidate); (2) 're', set to 1 for resolved objects in the SDSS images, set to 0 for non-resolved objects; (3) 'spec', set to 1 for objects with available follow-up spectroscopy, set to 0 for objects we did not follow-up; (4) 'phot', set to 1 for objects with available follow-up photometry, set to 0 for objects we did not follow-up; (5) 'segue', set to 1 if the considered WDMS binary was identified by our dedicated SEGUE survey, set to 0 otherwise.

(iii) *Manual search*. The user may run his own SQL scripts on the six tables introduced in Section 5.1. For example, if the user wishes to search for WDMS binaries identified as PCEBs with at least one of the Na I doublet radial velocity measurements above 100 km s^{-1}, no available photometric observations, SDSS *i* magnitudes of less than 18.5, with declinations between 0° and 30°, and white dwarf mass errors less than 0.1 $M_{\odot}$, the user should type the following:

```
select
s.iau_name, s.mwde, f.i, p.rv_na
from
mean_param as s, rv as p, magnitudes as f
where
s.iau_name = p.iau_name
and s.iau_name = f.iau_name
and p.rv_na > 100
```

and s.sigma > 0
and phot = 0
and Mwde between 0.0001 and 0.1
and f.i < 18.5
and f.decl between 0 and 30

6 SUMMARY

We have identified 646 new spectroscopic SDSS WDMS binaries; 395 have been detected within the spectroscopic SDSS I/II Legacy Survey, the remaining 251 new discoveries result from an efficient (64 per cent success rate) survey carried out by us within SEGUE. This survey has been designed to detect a population of WDMS binaries containing cold white dwarfs and/or early-type companion stars, a population of WDMS binaries clearly under-represented in all previous WDMS binary samples. The total number of spectroscopic SDSS WDMS binaries increased to 2248, and we expect this final DR7 SDSS WDMS binary catalogue to be $\gtrsim$98 per cent complete. Using an updated version of our decomposition/fitting routine, we have determined/updated the stellar parameters of the complete SDSS WDMS binary catalogue. Comparing the parameter distributions of the SDSS I/II and SEGUE WDMS binary samples, we demonstrated that our SEGUE survey indeed has been very efficient at identifying WDMS binaries containing cold white dwarfs. The DR7 WDMS binary catalogue represents the largest and most homogeneous sample of compact binary stars presented so far and an excellent basis for further follow-up studies. This potential can now be explored easily using our new user-friendly interactive online data base of SDSS WDMS binaries containing all available stellar parameters, radial velocities and magnitudes, now publicly available at http://www.sdss-wdms.org/.

ACKNOWLEDGMENTS

AR-M and MRS acknowledge financial support from Fondecyt in the form of grant numbers 3110049 and 1100782, respectively. ANG-M acknowledges support by the Centre National d'Etudes Spatial (CNES, ref. 60015). We thank Ivan Almonacid for his contributions to the development of the SQL data base. We thank Rene Heller for helpful discussions.

REFERENCES

Abazajian K. N. et al., 2009, ApJ, 182, 543
Adelman-McCarthy J. K. et al., 2008, ApJS, 175, 297
Althaus L. G., Benvenuto O. G., 1997, ApJ, 477, 313
Bergeron P., Wesemael F., Beauchamp A., 1995, PASP, 107, 1047
Catalán S., Isern J., García-Berro E., Ribas I., 2008, MNRAS, 387, 1693
de Kool M., 1992, A&A, 261, 188
De Marco O., Passy J.-C., Moe M., Herwig F., MacLow M.-M., Paxton B., 2011, MNRAS, 411, 2277
Dye S. et al., 2006, MNRAS, 372, 1227
Farihi J., Becklin E. E., Zuckerman B., 2005, ApJS, 161, 394
Farihi J., Hoard D. W., Wachter S., 2010, ApJ, 190, 275
Fontaine G., Brassard P., Bergeron P., 2001, PASP, 113, 409
Hauschildt P. H., Baron E., 1999, J. Comput. Applied Math., 109, 41
Heller R., Homeier D., Dreizler S., Østensen R., 2009, A&A, 496, 191
Hewett P. C., Warren S. J., Leggett S. K., Hodgkin S. T., 2006, MNRAS, 367, 454
Iben I. J., Livio M., 1993, PASP, 105, 1373
Iben, I., Jr, Tutukov A. V., 1986, ApJ, 311, 742
Jordi K., Grebel E. K., Ammon K., 2006, A&A, 460, 339
Koester D., Napiwotzki R., Voss B., Homeier D., Reimers D., 2005, A&A, 439, 317
Koester D., Kepler S. O., Kleinman S. J., Nitta A., 2009, J. Phys. Conf. Ser., 172, 012006
Lawrence A. et al., 2007, MNRAS, 379, 1599
Li N., Thakar A. R., 2008, Comput. Sci. Eng., 10, 18
Martin D. C. et al., 2005, ApJ, 619, L1
Morrissey P. et al., 2005, ApJ, 619, L7
Nebot Gómez-Morán A. et al., 2009, A&A, 495, 561
Nebot Gómez-Morán A. et al., 2011, submitted
Paczynski B., 1976, in Eggleton P., Mitton S., Whelan J., eds, Proc. IAU Symp. 73, Structure and Evolution of Close Binary Systems. Reidel, Dordrecht, p. 75
Parsons S. G., Marsh T. R., Copperwheat C. M., Dhillon V. S., Littlefair S. P., Gänsicke B. T., Hickman R., 2010, MNRAS, 402, 2591
Parsons S. G. et al., 2011, MNRAS (doi:10.1111/j.1365-2966.2011.19691.x)
Pickles A. J., 1998, PASP, 110, 863
Pyrzas S. et al., 2009, MNRAS, 394, 978
Pyrzas S. et al., 2011, preprint (arXiv e-prints)
Raymond S. N. et al., 2003, AJ, 125, 2621
Rebassa-Mansergas A., Gänsicke B. T., Rodríguez-Gil P., Schreiber M. R., Koester D., 2007, MNRAS, 382, 1377
Rebassa-Mansergas A. et al., 2008, MNRAS, 390, 1635
Rebassa-Mansergas A., Gänsicke B. T., Schreiber M. R., Koester D., Rodríguez-Gil P., 2010, MNRAS, 402, 620
Rebassa-Mansergas A., Nebot Gómez-Morán A., Schreiber M. R., Girven J., Gänsicke B. T., 2011, MNRAS, 413, 1121
Rechenberg I., 1994, Evolutionsstrategie '94. Froomann–Holzboog, Stuttgart
Richards G. T. et al., 2002, AJ, 123, 2945
Schreiber M. R., Gänsicke B. T., 2003, A&A, 406, 305
Schreiber M. R., Nebot Gómez-Morán A., Schwope A. D., 2007, in Napiwotzki R., Burleigh M. R., eds, ASP Conf. Ser. Vol. 372, 15th European Workshop on White Dwarfs. Astron. Soc. Pac., San Francisco, p. 459
Schreiber M. R., Gänsicke B. T., Southworth J., Schwope A. D., Koester D., 2008, A&A, 484, 441
Schreiber M. R. et al., 2010, A&A, 513, L7
Silvestri N. M. et al., 2006, AJ, 131, 1674
Silvestri N. M. et al., 2007, AJ, 134, 741
Smolčić V. et al., 2004, ApJ, 615, L141
Strauss M. A. et al., 2002, AJ, 124, 1810
Tuffs R. J., Popescu C. C., Völk H. J., Kylafis N. D., Dopita M. A., 2004, A&A, 419, 821
Warren S. J. et al., 2007, MNRAS, 375, 213
Webbink R. F., 1984, ApJ, 277, 355
West A. A., Hawley S. L., Bochanski J. J., Covey K. R., Reid I. N., Dhital S., Hilton E. J., Masuda M., 2008, AJ, 135, 785
Willems B., Kolb U., 2004, A&A, 419, 1057
Yanny B. et al., 2009, AJ, 137, 4377
York D. G. et al., 2000, AJ, 120, 1579
Zorotovic M., Schreiber M. R., Gänsicke B. T., NebotGómez-Morán A., 2010, A&A, 520, A86
Zorotovic M., Schreiber M. R., Gänsicke B. T., 2011, preprint (arXiv e-prints)

APPENDIX A: EXCERPTS OF SQL TABLES

We provide here excerpts for the six tables on our interactive online data base. The complete tables are available at http://www.sdss-wdms.org/.

Table A1. Table 'object'. It contains the identification number (ID) and abbreviated name for the complete catalogue.

ID	Abbreviated name
0001	SDSS J0001+0006
0002	SDSS J0004−0020
0003	SDSS J0006+0034
0004	SDSS J0010+0031
0005	SDSS J0012+0010

Table A2. Table 'object_iau_name'. It contains the identification number (ID) and international astronomical union name for the complete catalogue.

ID	IAU name
0001	SDSS J000152.09+000644.7
0002	SDSS J000442.00−002011.6
0003	SDSS J000611.93+003446.5
0004	SDSS J001029.87+003126.2
0005	SDSS J001247.18+001048.7

Table A3. Table 'rv'. It contains the measured Na I absorption doublet and Hα emission radial velocities and corresponding errors, together with the Heliocentric Julian Dates (HJD) of the observations and the telescope used for obtaining the spectra. We indicate by '–' that no radial velocity values are available.

IAU name	HJD	RV_{Na} ($km\,s^{-1}$)	Error ($km\,s^{-1}$)	$RV_{H\alpha}$ ($km\,s^{-1}$)	Error ($km\,s^{-1}$)	Telescope
SDSS J000152.09+000644.7	2451791.8092	0.70	21.10	24.20	16.70	SDSS
SDSS J001247.18+001048.7	2452519.8962	–	–	12.30	18.60	SDSS
SDSS J001247.18+001048.7	2452518.9219	−14.30	30.10	30.60	14.40	SDSS
SDSS J001359.39−110838.6	2452138.3933	28.90	16.90	0.00	0.00	SDSS
SDSS J001726.63−002451.1	2452559.7852	−33.70	15.50	−30.10	11.40	SDSS

Table A4. Table 'magnitudes'. It contains the right ascensions and declinations, as well as the ultraviolet *GALEX* DR6, SDSS and near-infrared UKIDSS DR6 magnitudes plus photometric errors. We indicate by '–' that no magnitudes are available. The errors have not been included here but are available at http://www.sdss-wdms.org/.

IAU name	RA (°)	Dec. (°)	NUV	FUV	*u*	*g*	*r*	*i*	*z*	*y*	*J*	*H*	*K*
SDSS J000152.09+000644.7	0.467 04	0.112 42	18.458	17.903	19.031	18.617	17.946	17.501	17.251	16.513	16.059	15.401 60	15.289
SDSS J000442.00−002011.6	1.175 00	−0.336 56	–	–	23.723	20.389	19.138	18.656	18.284	–	–	–	–
SDSS J000611.93+003446.5	1.549 75	0.579 58	21.780	0.000	21.383	20.926	20.129	19.005	18.381	17.536	17.056	16.580 58	16.201
SDSS J001029.87+003126.2	2.624 46	0.523 94	20.178	19.964	21.929	20.853	19.975	19.001	18.421	17.659	17.147	16.528 21	16.363
SDSS J001247.18+001048.7	3.196 58	0.180 19	20.509	20.711	20.734	20.216	19.664	18.634	17.965	17.093	16.601	16.133 05	0.000

Table A5. Table 'wdms'. It contains the stellar parameters for both components, the identifiers for SDSS spectra (MJD, PLT, FIB), and spectral types of our WDMS binaries (see Rebassa-Mansergas et al. 2010 for a description). The secondary star masses and radii (M_{sec} and R_{sec}) are obtained from the Sp–M–R relation by Rebassa-Mansergas et al. (2007). We provide two white dwarf solutions as obtained from our decomposition/fitting routine. The adopted solution is given by 1 in the first column and the ruled out solution by 0. The error parameters have not been included here but are accessible at http://www.sdss-wdms.org/.

Solution	IAU name	Type	MJD	PLT	FIB	T_{eff}(wd) (K)	log *g*	M_{wd} ($M_\odot$)	R_{wd} ($R_\odot$)	d_{wd} (pc)	Sp	M_{sec} ($M_\odot$)	R_{sec} ($R_\odot$)	d_{sec} (pc)
1	SDSS J001726.63−002451.1	DA/M	52559	1118	280	15 601	7.800	0.510	0.014 79	504	4	0.319	0.326	477
0	SDSS J001726.63−002451.1	DA/M	52559	1118	280	12 681	8.060	0.640	0.012 43	345	4	0.319	0.326	477
1	SDSS J001726.63−002451.2	DA/M	52518	0687	153	13 588	8.110	0.680	0.012 03	374	4	0.319	0.326	503
0	SDSS J001726.63−002451.2	DA/M	52518	0687	153	15 422	8.050	0.640	0.012 58	418	4	0.319	0.326	503
1	SDSS J001733.59+004030.4	DA/M	51795	0389	614	10 918	7.180	0.270	0.022 15	695	4	0.319	0.326	469
0	SDSS J001733.59+004030.4	DA/M	51795	0389	614	11 302	6.860	0.200	0.027 26	856	4	0.319	0.326	469

Table A6. Table 'mean_param'. It contains average stellar parameters for both stellar components, as well as WDMS binary spectral types (see Rebassa-Mansergas et al. 2010 for a description) and PCEB orbital periods. The secondary star masses and radii ($M_{\rm sec}$ and $R_{\rm sec}$) are obtained from the Sp–M–R relation by Rebassa-Mansergas et al. (2007). To identify PCEBs and wide WDMS binaries the column 'sigma' is set to 3 and 4 (representing 3σ and 4σ radial velocity variations), and 0 respectively, otherwise it is set to −1. To identify resolved objects we set the column 're' to 1, and it is set to 0 for unresolved objects. To identify objects followed up by our own team we set 'phot' and 'spec' to 1 if those have been observed photometrically and spectroscopically, respectively, and set to 0 otherwise. To identify WDMS binaries identified by our SEGUE survey we set 'segue' to 1, and 0 otherwise. Note also that the errors have not been included here but are available at http://www.sdss-wdms.org/.

IAU name	Type	$T_{\rm eff}$(wd) (K)	log g	$M_{\rm wd}$ ($M_\odot$)	$R_{\rm wd}$ ($R_\odot$)	$d_{\rm wd}$ (pc)	Sp	$M_{\rm sec}$ ($M_\odot$)	$R_{\rm sec}$ ($R_\odot$)	$d_{\rm sec}$ (pc)	sigma	$P_{\rm orb}$ (h)	phot	spec	re	segue
SDSS 013335.54+130357.1	DA/M	29 052	7.955	0.665	0.014 81	1626	2	0.431	0.445	1252	0	0	0	1	0	0
SDSS J013356.07−091535.1	DA/M	12 250	7.360	0.320	0.019 70	573	8	0.120	0.114	247	−1	0	0	0	0	0
SDSS J013418.52+010100.0	DA/M	23 343	7.710	0.490	0.016 08	1022	1	0.464	0.480	1146	−1	0	0	0	1	0
SDSS J013441.30−092212.7	WD/M	12 110	7.050	0.240	0.024 46	2357	2	0.431	0.445	1907	−1	0	0	0	0	0
SDSS J013504.31−085919.0	DA/M	9401	9.060	1.230	0.005 38	169	4	0.319	0.326	471	−1	0	0	0	0	0
SDSS J013716.08+000311.3	DA/M	19 193	8.390	0.860	0.009 83	643	2	0.431	0.445	856	0	0	0	1	0	0

This paper has been typeset from a TEX/LATEX file prepared by the author.